Biointerface Research in Applied Chemistry
Open-Access Journal (ISSN: 2069-5837)

Article
Volume 14, Issue 2, 2024, 48
https://doi.org/10.33263/BRIAC142.048

Network Pharmacology Approach and Molecular Docking Prediction to Investigate the Possible Mechanism of Benzylidene Derivatives Against Scavenging Reactive Oxygen Species via Sirtuin 3 in Parkinson's Disease

Gomathy Subramanian [1], Srikanth Jupudi [1], Jagdish Chand [1,*], Mohammad Zubair Baba [1], Aryan [1]

[1] Department of Pharmaceutical Chemistry, JSS College of Pharmacy, JSS Academy of Higher Education & Research, Ooty-643001, The Nilgiris, Tamil Nadu, India Tel- +91-423-2443393 (Ext-218) Fax- +91-4232442937
* Correspondence: sachinchand190@gmail.com;

Scopus Author ID 58034695100
Received: 13.04.2023; Accepted: 28.05.2023; Published: 4.02.2024

Abstract: Benzylidene derivatives have been extensively used to treat Parkinson's disease (PD). Various *in-vitro* and *in-vivo* studies on benzylidene have been shown to reduce oxidative stress and have resulted in neuroprotective effects. In addition, the mechanism of action of the therapeutic agents used in treating PD is unclear. Therefore, this study aims to investigate the potential molecular pathways behind antiparkinsonian activity by employing a network pharmacology approach.Various open-source databases were used in the designing of benzylidene derivatives. The virtual screening was performed for the hit-designed compounds by the putative targets implicated in PD development. The drug-likeness score, ADMET studies, and probable adverse effects were also predicted using admet SAR 2.0 and ADVERpred database. The regulated pathways were predicted using the Kyoto Encyclopedia of Genes database (KEGG). Among the designed 10 compounds (BH-1 to BH-10), the BH-1 compound was found to modulate proteins that are implicated in the progression of PD using Cytoscape 3.7.2. The further conformational analysis of the compounds was performed using molecular docking, MMGBSA, and molecular dynamics studies using the Schrödinger suite 2022. The designed compound BH-1 was determined to have the highest number of edge counts and was determined to have the highest docking score of -7.463 kcal/mol, with the highest MMGBSA score of -59.55 kcal/mol. Further, the network between the designed compounds, pathway, and gene, the FoxO signaling pathway, was found to be the most regulated pathway. The newly designed compounds have been found to exhibit significant potent results as compared to the standard molecule resveratrol. The findings suggested that the designed compound BH-1 could be a potential therapeutic agent in the treatment of PD.

Keywords: Parkinson's disease; FoxO signaling pathway; Benzylidene derivatives; Network-pharmacology; *in-silico* studies

1. Introduction

The loss of dopaminergic neurons in the substantia nigra (SN) of the brain is a hallmark of Parkinson's disease (PD); effective treatment requires synthetic molecules [1]. These neuroprotective molecules can produce psychosis and hallucinations by generating an abundance of reactive oxygen species (ROS) that disrupt mitochondrial activity [2]. PD is a polygenic disease, indicating several genes involved in its onset. When one protein's function is altered, many other pathways are substantially activated, which has synergistic effects on the

disease process. It suggests the presence of several genes that cooperate to produce a certain effect. Antiparkinsonian medications increasingly target specific targets from a variety of drug target mechanisms implicated in the pathophysiology of Parkinson's disease; a central *"selective drug target strategy"* may have polypharmacological effects [3]. Parkinson's disease is a multifaceted, progressive neurodegenerative condition; using the "*multiple protein drug approach*" in low dose concentration is preferable to have a substantial effect. Numerous neuroprotective properties of synthetic molecules have been reported, including the capacity to raise dopamine levels in the SN while causing minimal adverse effects [4]. The synthesis of ATP, $Ca2^{+}$ homeostasis, the tricarboxylic acid cycle (TCA), and ROS regulation are all regulated by the protein deacetylase sirtuin 3 (SIRT3), which is dependent on nicotinamide adenine dinucleotide (NAD+); the Krebs cycle, peroxisome proliferator-activated receptor-Coactivator (PGC-1), and estrogen-related receptor are all affected by mitochondrial dysfunctioning because of faulty functioning of these proteins, which leads to excess production of ROS and leads to neuronal death [5]. Numerous antioxidants are also involved in controlling reactive oxygen species (ROS), which prevents the degeneration of dopaminergic neurons. These include superoxide dismutase 2 (SOD2) and forkhead box (FOXO1) [6]. Several studies have shown that the substantia nigra of the brain, which houses the dopaminergic neurons, has damaged mitochondria and an altered mitochondrial respiratory chain (MRC), both of which could lead to excessive production of reactive oxygen species (ROS) and neurodegeneration [7]. This study focuses on several benzylidene-based hydroxy derivatives derived from phenyl methanol with various substitutions. Hereby, many *in-silico* studies have demonstrated that benzylidene-based hydroxy derivatives are superior to the gold standard molecules in suppressing ROS generation and fostering healthy mitochondrial biogenesis.

2. Materials and Methods

2.1. Preparation of the ligands and proteins genes involved in the PD.

The Chem Draw 19.0 and maestro LigPrep module in Schrödinger suite 2022 were used in the preparation of the eleven substituted benzylidene-based hydroxy derivatives (BH-1 to BH-11). The prepared ligands were then transformed into a useful database that included SMILES and other physiochemical properties. The molecules were extracted using the ZINC database (https://zinc.docking.org/). The Swiss Target Prediction database (http://www.swisstargetprediction.ch/) was queried for potential targets with a 70–90% similarity rate for the individual molecule [8]. To identify the common targets, the target genes were identified from the Therapeutic Target Database (http://db.idrblab.net/ttd/), and the Gene IDs were collected from the UniProt database (https://www.uniprot.org).

2.2. Druglikness and ADMET profiling of the designed ligands.

The "Lipinski rule of Five methods" in MolSoft (https://www.molsoft.com/) was used to evaluate drug-likeness ratings. The compound's ADMET profiles were determined using admetSAR2.0 (http://lmmd.ecust.edu.cn/admetsar2) [9]. Furthermore, the QikProp module in Schrödinger Suite 2022 was used to obtain the ADME study for the designed compounds.

2.3. Identification of Adverse effects.

The Potential adverse effects were predicted using the designed compounds SMILES and the ADVERpred database (http://www.way2drug.com/adverpred/) [10]. Analysis was done on probable activity (Pa) and probable inactivity (Pi) values. If the Pa value was discovered to be higher than the Pi value, the phytoconstituent adverse effects were taken into account while maintaining the value of 0.8.

2.4. Identification of protein pathways and construction of the network.

The STRING database (https://string-db.org/) was used to analyze the collected genes further to determine the network of protein-protein interactions involved in the development of PD [11]. Additionally, the KEGG pathway database (https://www.genome.jp/kegg/) was used to identify the proteins and regulated pathways associated with PD. The supplementary file Table No. S1 contains all of the resulting pathways. Using Cytoscape 3.7.2, a network was built between the target genes, pathways, and compounds [12].

2.5. Docking studies.

The Schrödinger suite 2022 was used for molecular docking experiments. BH-1 to BH-11 was generated as a three-dimensional structure using the ligand designer maestro tool. The LigPrep module was then used to create these structures with a pH range of 7.4. The compound's energy was reduced using the Epik module, and the force field employed was OPLS3 [13]. The protein data bank (https://www.rcsb.org/) provided the human SIRT3 bound to Ac-ACS peptide with the PDB ID: 4FVT. Utilizing the protein preparation workflow tool of the Schrödinger suite 2022, the protein was replenished with the missing hydrogens, water, and amino acids. The grid box was generated using the glide and receptor grid-generating modules. Molecular docking was performed with great precision using the ligand docking module from the Schrödinger suite 2022 (XP) [14].

2.6. Molecular Dynamics.

To verify the stability of compound BH-1 and protein interaction at 100 nanoseconds time intervals, a detailed molecular dynamics simulation study was carried out in the Desmond program of Schrödinger suite 2022. The BH-1 interacted with atoms and the protein's structural core. It was discovered that the BH-1 docking score was the highest among all the designed compounds. The root mean square deviation (RMSD) of the ligand-protein complex reached a continuous peak between 20 and 100 nanoseconds.

3. Results

3.1. De novo drug design and extraction of the proteins involved in the PD.

In this approach, novel compounds were developed based on molecular shape and converted into input SMILES, as shown in Supplementary file Table S2. The active site of the proteins was predetermined, and the structure-based De novo drug creation process was devised. Supplementary file-Figure S1 shows that the designed compounds were further generated using the LigPrep module in Schrödinger suite 2022. Several PD proteins were found to be modulated by the eleven proposed compounds; these modulated proteins were located by

querying the Swiss Target Prediction Database using the compounds SMILES. Table 1 summarizes the proteins that were modulated by the proposed compounds.

Table 1. Designed benzylidene-based hydroxymethyl derivatives and their modulated targets.

Compounds code	Substituted (R) Aldehydes	Compound	Targeted Proteins (Genes)
BH-1	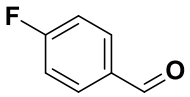	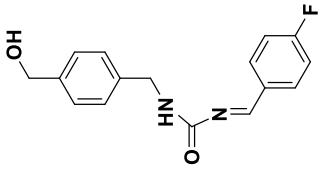	ADORA1, NTRK1, NTRK3, PRKDC, HIF1A, CDC34, HSD11B1, PRKAA2, ATP5B, HDAC1, SOD2, FOXO1, PPARGC1A, UBB, AMPK, IDH2, SIRT3
BH-2	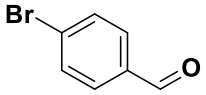	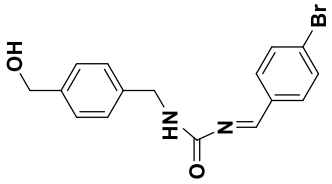	PRKAA2, ATP5B, HDAC1, SOD2, FOXO1, PPARGC1A, UBB, NTRK1, HMGCR, HIF1A, EPHX2, AMPK, SIRT3l, ALOX5
BH-3	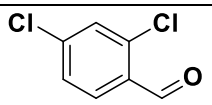	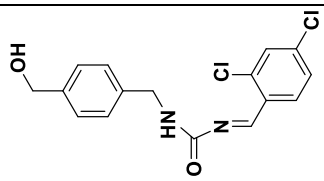	PRKAA2, HDAC1, SOD2, FOXO1, PPARGC1A, AMPK, IDH2, NTRK2, CREBBP, SIRT3, MAP2K1, HMGCR, ALOX5
BH-4	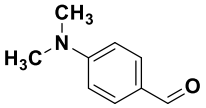	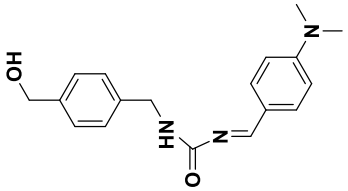	HSD11B1, PRKAA2, ATP5B, HDAC1, SOD2, FOXO1, PPARGC1A, UBB, AMPK, IDH2, NTRK2, EPHX2, CREBBP, SIRT3, MAP4K4, HMGCR, ALOX5
BH-5	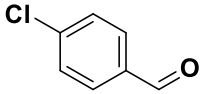	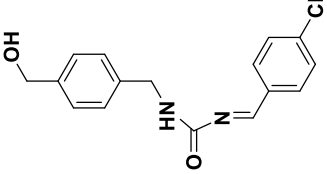	PRKAA2, ATP5B, HDAC1, SOD2, FOXO1, PPARGC1A, UBB, AMPK, IDH2, NTRK2, CREBBP, SIRT3, ALOX5
BH-6	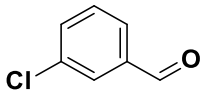	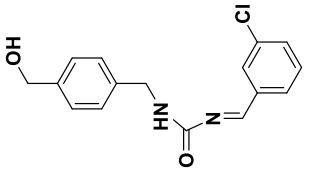	CDC34, HSD11B1, PRKAA2, ATP5B, HDAC1, SOD2, FOXO1, PPARGC1A, UBB, AMPK, IDH2, NTRK2, CREBBP, SIRT3
BH-7	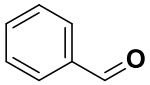	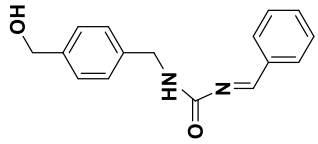	SOD2, NTRK2, CREBBP, SIRT3, CDK1, PDE2A, FOXO1, PPARGC1A
BH-8	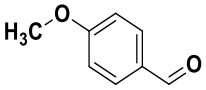	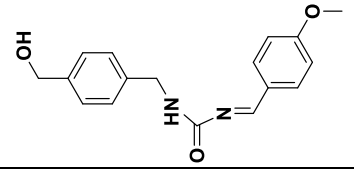	CDC34, PRKAA2, ATP5B, HDAC1, SOD2, NTRK2, CREBBP, FOXO1, PPARGC1A, UBB, AMPK, IDH2, MAP4K4, SIRT3, ALOX5
BH-9	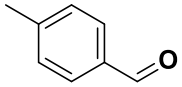	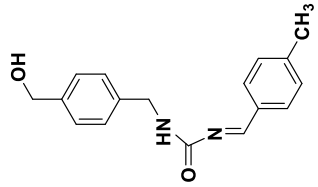	PRKAA2, ATP5B, HDAC1, SOD2, FOXO1, PPARGC1A, SIRT3, NTRK2, CREBBP, ALOX5

Compounds code	Substituted (R) Aldehydes	Compound	Targeted Proteins (Genes)
BH-10	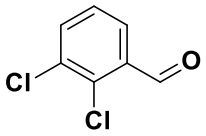	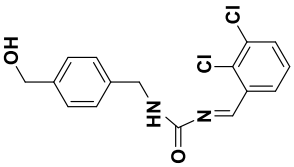	NTRK2, CREBBP, CDC34, PRKAA2, ATP5B, HDAC1, SOD2, FOXO1, PPARGC1A, AMPK, IDH2, SIRT3
BH-11	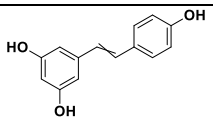	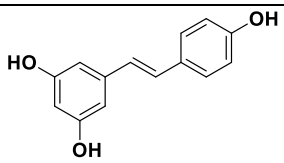	PTGS1, CA1, ALOX5, RELA, ESRRB, IGF1R, CDC34, HSD11B1, PRKAA2, ATP5B, HDAC1, SOD2, SIRT3, NTRK2, CREBBP

3.2. Probable adverse effects, drug-likeness of designed compounds, and ADMET study.

The potential levels of activity (Pa) and inactivity (Pi) were used to evaluate all of the developed compound's potential adverse effects, as shown in Figure 1. For compound BH-1, hepatotoxicity was determined to be the least likely side effect; nevertheless, for compounds BH-2 through BH-11, myocardial infarction and nephrotoxicity were detected. Resveratrol, a common chemical, showed a potential negative influence on arrhythmia, which is depicted in Figure 1. Additionally, the drug-likeness of all fifteen substances (BH-1 to BH-11) was evaluated; Table 2 shows that BH-1 had the highest drug-likeness score. As depicted in Figure 2. Blood-brain barrier permeability, mitochondrial toxicity, human oral bioavailability, plasma protein interaction, and human intestinal absorption were all examined for the proposed drugs.

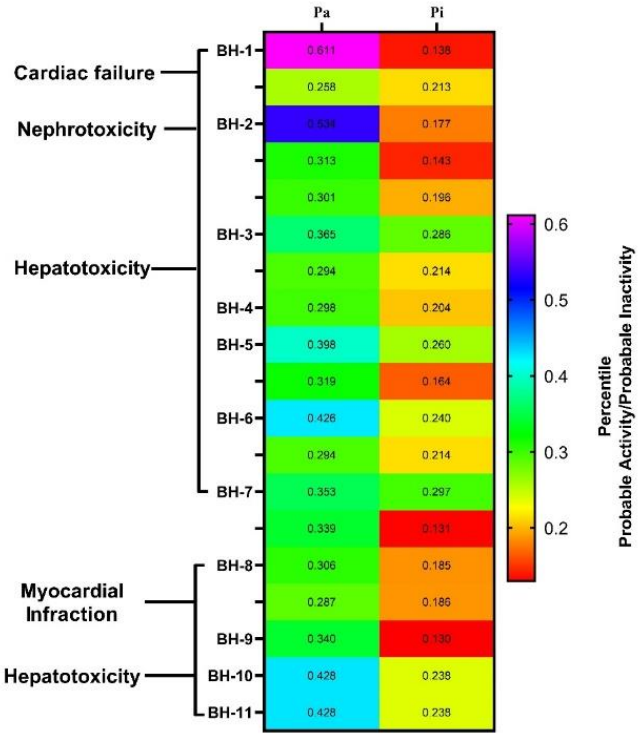

Figure 1. The probable adverse effects of all the designed compounds based on their; Pa: Probable activity; Pi: Probable inactivity score.

Table 2. Druglikeness score and physicochemical properties of designed BH-1 to BH-11 compounds.

Compounds	Molecular formula	MW	NHBA	NHBD	Log P	Log S	DLS	QPlogBB
BH-1	$C_{16}H_{15}BrN_2O_2$	347.2	5.2	2	3.075	-4.4	0.41	-0.845
BH-2	$C_{16}H_{15}FN_2O_2$	286.1	5.2	2	2.903	-4.0	0.38	-0.859
BH-3	$C_{16}H_{14}Cl_2N_2O_2$	337.2	5.2	2	3.464	-4.8	0.03	-0.623
BH-4	$C_{18}H_{21}N_3O_2$	311.3	6.2	2	2.972	-4.6	0.41	-1.192
BH-5	$C_{16}H_{15}ClN_2O_2$	302.7	5.2	2	3.145	-4.8	0.00	-1.061
BH-6	$C_{16}H1_5ClN_2O_2$	302.7	5.2	2	3.149	-4.8	0.18	-1.064

Compounds	Molecular formula	MW	NHBA	NHBD	Log P	Log S	DLS	QPlogBB
BH-7	$C_{16}H_{16}N_2O_2$	268.3	5.2	2	2.27	-3.4	-0.5	-1.209
BH-8	$C_{17}H_{18}N_2O_3$	298.3	5.95	2	2.72	-4.4	0.38	-1.299
BH-9	$C_{17}H_{18}N_2O_2$	282.3	5.2	2	2.801	-4.2	0.41	-1.121
BH-10	$C_{16}H_{14}Cl_2N_2O_2$	337.2	5.2	2	3.445	-5.0	0.01	-0.842
BH-11	$C_{14}H_{12}O_3$	228.2	2.25	3	1.997	-2.7	-1.0	-1.272

MW Molecular weight, NHBA Number of Hydrogen Bond Acceptor, NHBD Number of Hydrogen Bond Donor, MolLogP (octanol/water partition coefficient), MolLogS (water solubility), DLS Druglikeness Score, QPlogBB Predicted brain/blood partition coefficien5

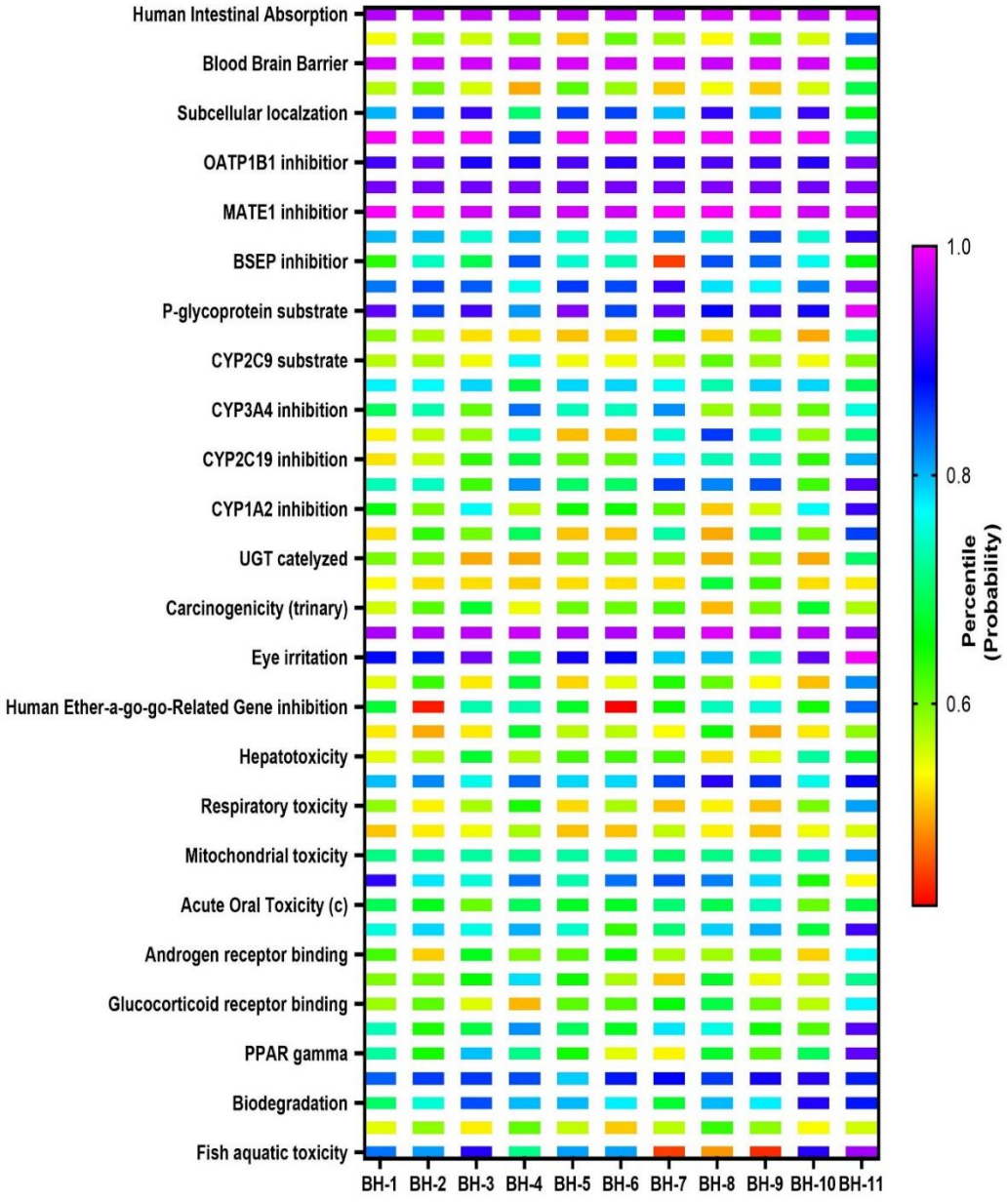

Figure 2. Screened ADMET profile of eleven designed benzylidene-3-(4-(hydroxymethyl) benzyl derivatives (BH-1 to BH-11).

3.3. Molecular Docking and Prime MMGBSA studies.

The compound BH-1 was found to have the highest binding affinity of -7.463 kcal/mol with the sirtuin 3 (PDB ID: 4FVT) among the eleven compounds BH-1 to BH-11. Furthermore, all eleven compounds remained to display their highest possible binding energies when the rank of the ligands was rearranged using the MMGBSA module in Schrödinger suite 2022. The MMGBSA score for the compound BH-1, which was found to be -59.55 kcal/mol, which was found to have the highest score. In Figure. 3, the interaction of the compound BH-1 with the

amino acids ARG 152, ASP 231, and PHE 180 is shown in two and three dimensions. In the supplementary file, Figure S2, and supplementary file, Figure S3, additional BH-2 to BH-10 and resveratrol binding interactions are depicted. The molecular binding affinity as compared to standard molecule resveratrol (BH-11), was found to be -5.04 kcal/mol with an MMGBSA score of -15.61 kcal/mol. The designed compound BH-1 was found to have the highest binding affinity in comparison to resveratrol, Figure 3 depicts the interaction of the resveratrol and the sirtuin 3 protein with various hydrogen bonding such as ILE 230, ILE 154, PHE 294, PHE 180, HIS248, VAL 292, and PRO 155 amino acids. The binding interactions of other compounds are depicted in the supplementary file, Table. S3.

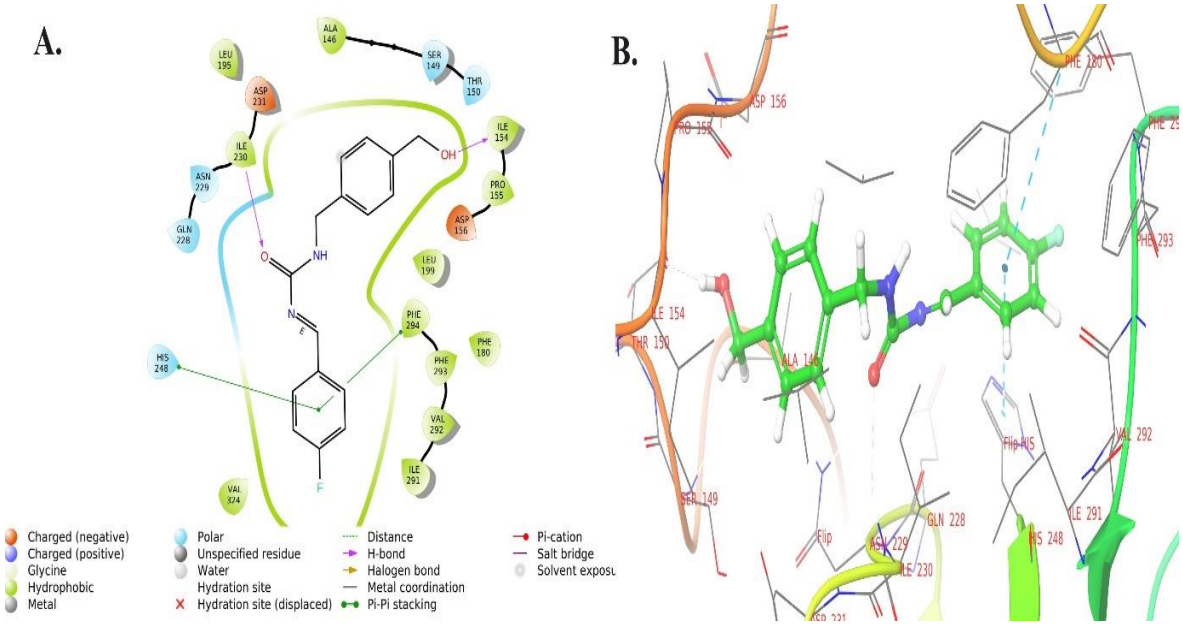

Figure 3. **(A**). The two-dimensional structure of the compound BH-1 with the sirtuin 3 protein. **(B).** The three-dimensional structure of the compound BH-1 with the sirtuin 3. The interactions show significant amino acids which are required in the proper functioning of the protein sirtuin 3. The PDB ID used to determine the amino acid interaction and the compound was PDB ID:4FVT.

3.4. Molecular Dynamics

At a speed of 100 nanoseconds, Desmond's Schrodinger suite 2022 molecular dynamics simulation analysis was utilized to validate the stability of the interaction between compound (E)-1-(4-fluorobenzylidene)-3-(4-(hydroxymethyl)benzyl)urea (BH-1) and protein. When developing the complex file that describes the ligand-protein interaction, we made use of the OPLS4 force field that is contained within the system builder module. According to the values, the interaction between the ligand and the protein became steady at around 20 nanoseconds, and it remained constant throughout. The SIRT3/ BH-1 complex was evaluated, and the results showed that its mean RMSD value was 2.4 Å as shown in Figure 4 (A). The SIRT3/BH-1 complex displayed the hydrogen interactions of SER 149, PHE 157, ARG 158, SER 159, ILE 230, and ASP 231. In addition to the demonstrated outcome, the interaction between SIRT3/BH-1 resulted in hydrophobic interactions with ALA 146, ILE 154, PRO 155, ARG 158, PHE 180, LEU 199, TYR 204, and HIS 248, which is shown in Figure 4. (B). It ensured the stability of the ligand in the active pocket of the SIRT3 throughout the complete molecular paths generated between the ligand and protein. In a nutshell, both ligand/protein complexes can form stable bonds.

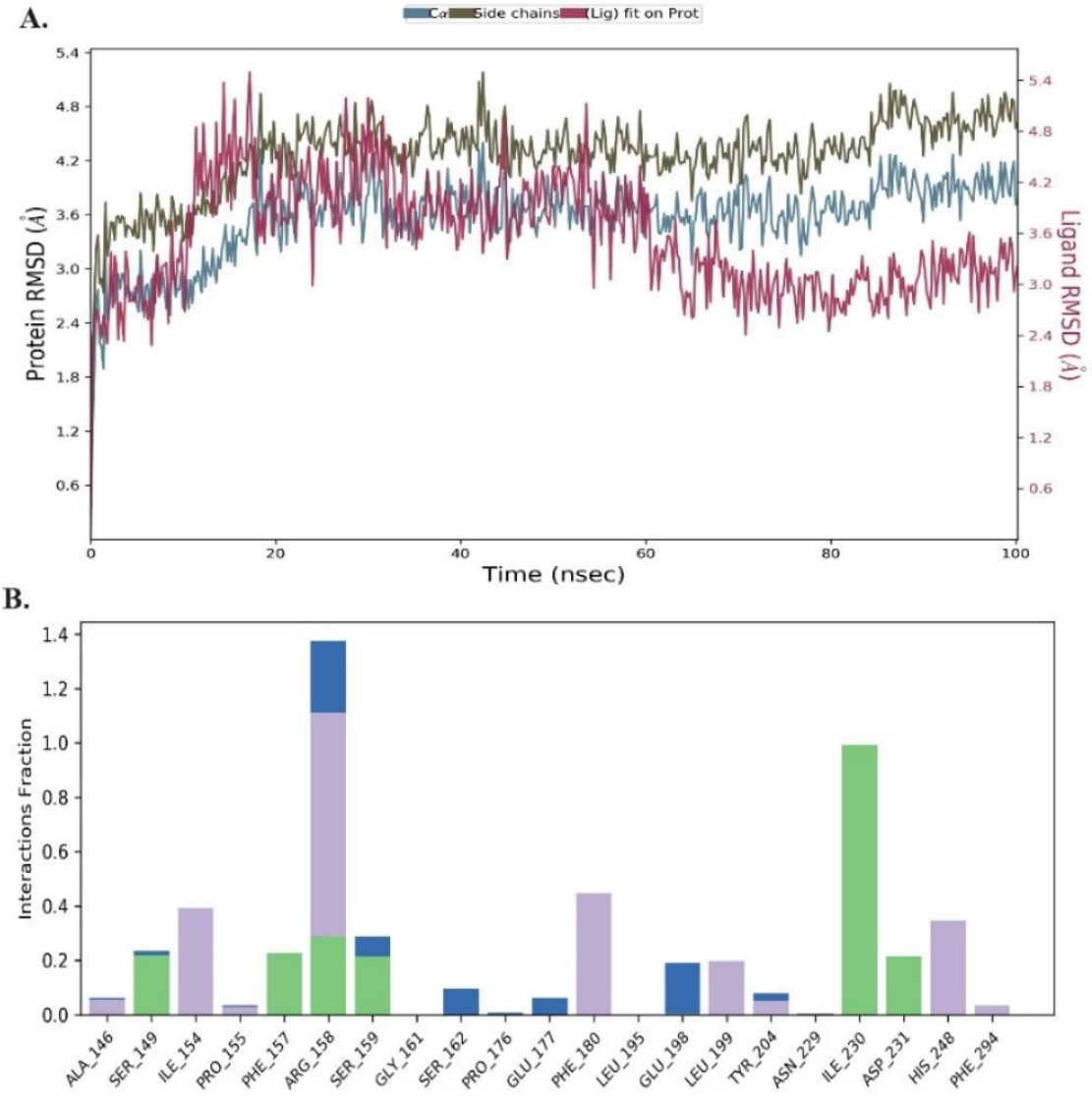

Figure 4. Root mean square deviation of MD studies. **(A)** RMSD plots of SIRT3 (PDB ID: 4FVT) and ligand (BH-1) at 100 ns. **(B)** Protein-ligand contact visualizing hydrogen bond interactions.

3.5. Analysis of pathways through the network.

The gene set enrichment analysis method identified 17 distinct pathways that were all regulated by genes implicated in the progression of Parkinson's disease. In addition, four pathways linked to the modulation of Parkinson's disease were found by the KEGG database gene enrichment analysis. The FoxO signaling pathway with the highest number of gene interactions was found to be the most active pathway, as shown in Table 3.

Table 3. Gene set enrichment of the pathways and proteins involved in PD.

Pathway	Description	Count In Gene Set	False Discovery Rate	Genes
hsa04068	FoxO signaling pathway	9	1.16	SIRT3, PRKAB1, CREBBP, PRKAA2, FOXO1, SOD2, PPARGC1A, SOD1, CREB1
hsa04152	AMPK signaling pathway	3	1.65	PPARGC1A, FOXO1, FOXO3
hsa04922	Glucagon signaling pathway	2	1.55	PPARGC1A, FOXO1
hsa04728	Dopaminergic synapse	4	0.0029	DRD4, MAOA, FOXO1, MAOB

The compound BH-1, which was discovered to have the greatest drug-likeness score and the highest docking score with the sirtuin 3 protein, as shown in Figure 5, was the objective of building the interaction network. Between compound BH-1, genes, and the regulated pathways, a network was established.

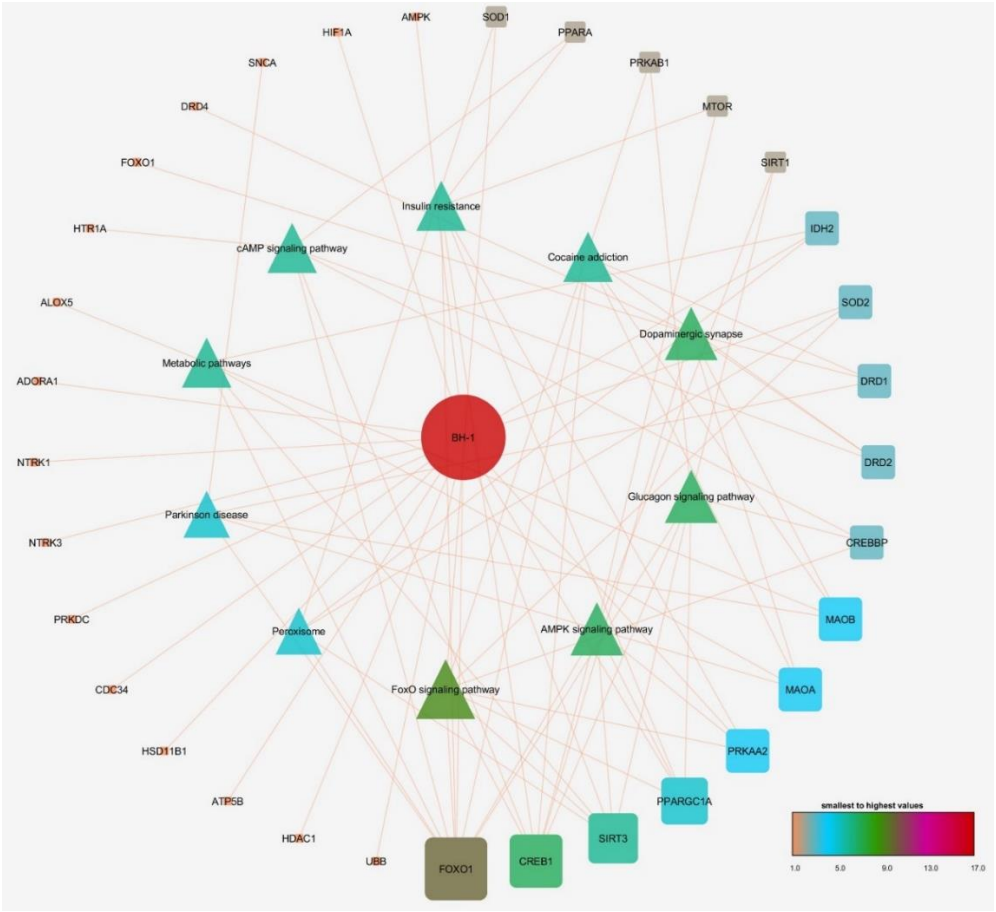

Figure 5. Network illustration between the designed compounds, pathways, and genes. The designed compound (E)-1-(4-fluorobenzylidene)-3-(4-(hydroxymethyl)benzyl)urea (BH-1) was found to modulate the FOXO signaling pathway and FOXO1 gene. The FOXO signaling pathway and FOXO1 gene have been found to reduce the reactive oxygen species and oxidative stress, which produce the neuroprotective effect.

The network analysis displayed 81 edge counts, among which 64 interactions were found between pathway-gene, and 17 counts were found between compound-pathway interactions. The compound BH-1 had the highest edge counts with 17 genes, namely ADORA1, NTRK1, NTRK3, PRKDC, HIF1A, CDC34, HSD11B1, PRKAA2, ATP5B, HDAC1, SOD2, FOXO1, PPARGC1A, UBB, AMPK, IDH2, and SIRT3 which were modulated via FOXO signaling pathway interactions. In compound BH-1 and FOXO signaling pathways, proteins such as SIRT3, FOXO1, and PPARGC1A were mostly modulated during the gene enrichment analysis.

3.6. Gene Ontology enrichment and pathways analysis.

The gene ontology enrichment analysis visualized 1015 biological processes, while the regulation of neuron death (GO:1901214) was found with the lowest false discovery rate by modulating 19 genes (SIRT1, CDC34, PPARGC1A, SOD1, NTRK2, UBB, SNCA, MTOR, FOXO1, ADORA1, NGF, PINK1, PPARA, CREB1, PARK7, CDK5, NTRK1, HIF1A, SOD2). Whereas 91 molecular functions were obtained, with the lowest false discovery rate,

the enzyme binding pathway (GO:0019899) was found to modulate 26 genes (NGFR, SIRT1, PRKAB1, SIRT2, MUL1, PPARGC1A, SOD1, NTRK2, PPARG, HMGCR, MAP2K1, UBB, PRKDC, MTOR, HDAC1, PINK1, FOXO1, SIRT3, RELA, PPARA, CREB1, PARK7, CDK5, ESRRB, NTRK1, HIF1A). Similarly, 61 cellular components were obtained among which neuron projection (GO:0043005) was found to modulate 27 genes (NGFR, DRD4, SIRT2, MUL1, PPARGC1A, IGF1R, SOD1, NTRK2, UBB, HTR1A, SNCA, NTRK3, MTOR, PTGS1, DRD2, ADORA1, NGF, PRKAA2, CNR2, PINK1, DRD1, CREB1, PARK7, CDK5, NTRK1, HTR2A, HIF1A), which have been displayed in Figure 6. In the current study, around 17 KEGG pathways were identified for Parkinson's disease with FoxO signaling pathway (hsa04068) modulating 9 genes (SIRT3, PRKAB1, CREBBP, PRKAA2, FOXO1, SOD2, PPARGC1A, SOD1, CREB1). The designed compound BH-1 had the greatest protein modulation and was directly involved in the modulation of PD in most pathways, as shown by the network interpretation of the compound.

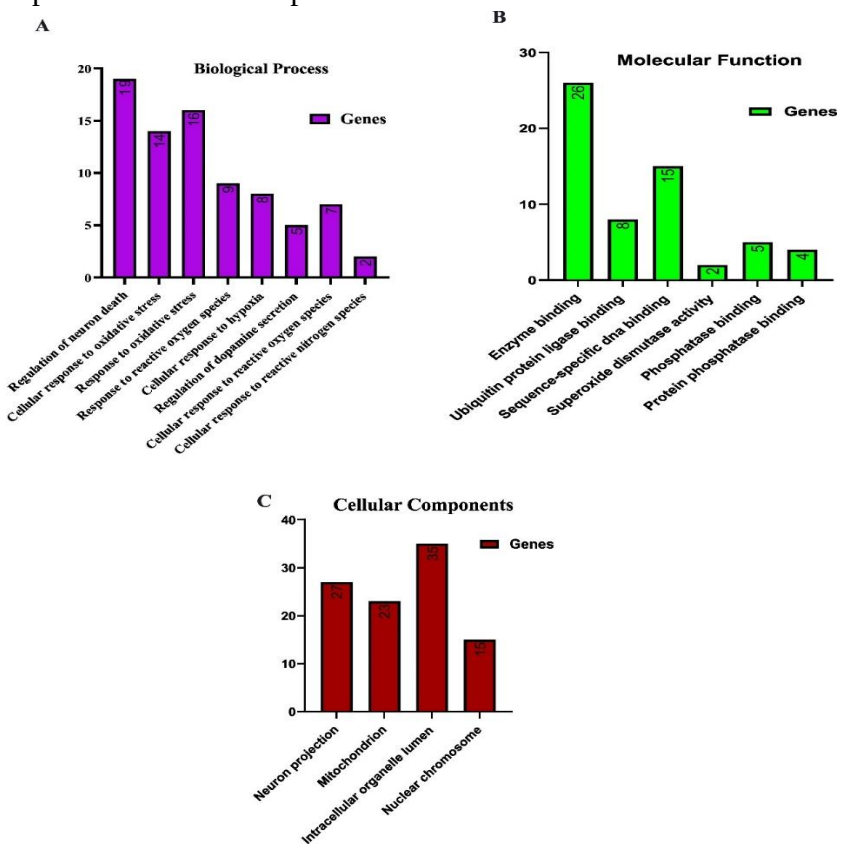

Figure 6. Gene ontology enrichment analysis of the pathways modulating various genes.

Notes: A. Biological process B. Molecular function C. Cellular function. Biological processes were found to have the highest number of regulated pathways and genes with the most likely pathways. The most highly modulated designed compound, BH-1, modulated a wide range of targets and genes, from which we were able to determine the likely pathways and gene count and from which we predicted that further modulation of those pathways might yield a neuroprotective impact.

4. Discussion

Appropriate therapeutic drugs, including resveratrol and levodopa, have been shown to have various detrimental effects based on long-term use, including fluctuations, dyskinesias, toxicity, or lack of efficacy in PD [15]. Computational approaches such as molecular docking

studies and network pharmacology approaches have resulted in well-established methods for PD [16]. Several decent studies have been conducted on how benzylidene-based hydroxy derivatives can be used to treat Parkinson's disease; the results showed that reactive oxygen species and oxidative stress were reduced, and the neuroprotective effect was enhanced [17]. In the current study, compound (E)-1-(4-fluorobenzylidene)-3-(4-(hydroxymethyl)benzyl)urea (BH-1) was found to be a potential modulator of the pathways involved in the progression of PD through networking. Among the designed benzylidene-based hydroxy derivatives, compound (E)-1-(4-fluorobenzylidene)-3-(4-(hydroxymethyl)benzyl)urea was found to have the highest binding affinity, which was determined using molecular docking studies. It should be noted that compound (E)-1-(4-fluorobenzylidene)-3-(4-(hydroxymethyl)benzyl)urea (BH-1), which was discovered to have significant interactions with other genes and where the various obtained pathways were found to regulate those genes, which might be a promising compound to produce neuroprotective effects and slow the progression of PD. In this study, the most highly regulated gene was FOXO1, the FoxO signaling pathway that suppresses reactive oxygen species and oxidative stress [18, 19]. The co-activation of FOXO1, CREB1, and PPARGC1A via SIRT3 may result in mitochondrial biogenesis, resulting in neuroprotection. Furthermore, gene set enrichment analysis using the KEGG pathway revealed four highly modulated pathways FoxO signaling pathway, AMPK signaling pathway, Glucagon signaling pathway, and Dopaminergic synapse, among which the FoxO signaling pathway (hsa04068) was found to be the most modulated pathway. FoxO signaling pathway was found to be the most common target found between the compound (E)-1-(4-fluorobenzylidene)-3-(4-(hydroxymethyl)benzyl)urea (BH-1), which is also involved in the regulation of reactive oxygen species and oxidative stress, as inactivation of FOXO may lead to upregulation of reactive oxygen species [20]. The relevance of this subfamily in mammalian lifespan is yet unknown, despite their involvement in a number of important physiological processes such as stress tolerance, metabolism, cell cycle arrest, and apoptosis [21]. The second most modulated AMPK signaling pathway/PPAR (peroxisome proliferator-activated receptor) (PGC-1α) coactivator, one pathway that controls mitochondrial biogenesis and is linked to the management of oxidative stress is the signaling pathway, where the PGG-1α is phosphorylated by AMPK signaling pathway and bind to Nrf1 and Nrf2 to promote proper mitochondrial biogenesis; whereas Nrf1 and Nrf2 preserve the mitochondrial biogenesis by regulating mitophagy [22]. Among the transcription factors and enzymes regulated by sirtuins are HIF-1, PGC-1α, FOXO1, PPAR, and others. Furthermore, sirtuins can modify mitophagy proteins like ATG5, ATG7, and ATG8 by contact with and/or post-translational modification. The designed compound (E)-1-(4-fluorobenzylidene)-3-(4-(hydroxymethyl)benzyl)urea (BH-1) and FOXO1 may make the dopaminergic neurons work and protect them through the FoxO signaling pathway. Our current study identified compound BH-1 as a prominent among the designed ten compounds that interacted with the maximum number of genes involved in the progression of PD. Further research on these findings is required to turn a potential study into compelling research.

5. Conclusions

The overproduction of reactive oxygen species may be caused by a number of circumstances, including increased metabolic activity, decreased antioxidant activity, excessive ROS production, or the ubiquitous nature of ROS as a by-product of cellular activity. Reduced levels of dopamine can result in a number of motor and non-motor symptoms,

including Parkinson's disease (PD), which is primarily caused by neurodegeneration or the death of neurons caused by an excess of reactive oxygen species in the brain. It has been discovered that benzylidene-based hydroxy derivatives such as resveratrol can successfully activate the sirtuin 3 gene, which plays a significant role in the process of mitochondrial biogenesis. The production of reactive oxygen species (ROS) as a consequence of mitochondrial dysfunction has been linked to neurodegeneration. Numerous studies have claimed the FoxO signaling pathway and FOXO1 as potent antioxidants that are involved in the downregulation of the reactive oxygen species, whereas upregulation of reactive oxygen species and dysfunctioning of the mitochondria is regarded as one of the main causes of PD. Our study marks compound (E)-1-(4-fluorobenzylidene)-3-(4-(hydroxymethyl)benzyl)urea (BH-1) as a potent modulator of the mentioned pathways and genes. On a note, the designed compounds can be used as antiparkinsonian agents.

Funding

The research was funded by JSS College of Pharmacy, JSS Academy of Higher Education & Research, Rocklands, Ooty, The Nilgiris, Tamilnadu, India. The award order number "JSSAHER/REG/RES/JSSURF/29(1)/2010-11".

Acknowledgments

We acknowledge the generous research infrastructure and support from JSS College of Pharmacy, JSS Academy of Higher Education & Research, Rocklands, Ooty, The Nilgiris, Tamilnadu, India.

Conflicts of Interest

The authors declare no conflicts of interest. The funders had no role in the study's design; in the collection, analyses, or interpretation of data; in the writing of the manuscript, or in the decision to publish the results.

References

1. Zaman, V.; Shields, D.C.; Shams, R.; Drasites, K.P.; Matzelle, D.; Haque, A.; Banik, N.L. Cellular and molecular pathophysiology in the progression of Parkinson's disease. *Metab. Brain Dis*, **2021**, *36*, 815–827, https://doi.org/10.1007/s11011-021-00689-5.
2. Tirozzi, A.; Modugno, N.; Palomba, N.P.; Ferese, R.; Lombardi, A.; Olivola, E.; Gialluisi, A.; Esposito, T. Analysis of Genetic and Non-genetic Predictors of Levodopa Induced Dyskinesia in Parkinson's Disease. *Front. Pharmacol.***2021**, *12*, 1-9, https://doi.org/10.3389/fphar.2021.640603
3. Cheong, S.L.; Federico, S.; Spalluto, G.; Klotz, K.N.; Pastorin, G. The current status of pharmacotherapy for the treatment of Parkinson's disease: transition from single-target to multitarget therapy. *Drug Discov. Today* **2019**, *24*, 1769–1783, https://doi.org/10.1016/j.drudis.2019.05.003
4. Zhang, Y.; Xu, X. Chinese Herbal Medicine in the Treatment of Depression in Parkinson's Disease: From Molecules to Systems. *Front. Pharmacol* **2022**, *13*, https://doi.org/10.3389/fphar.2022.879459
5. Sawa, K.; Uematsu, T.; Korenaga, Y.; Hirasawa, R.; Kikuchi, M.; Murata, K. Krebs cycle intermediates protective against oxidative stress by modulating the level of reactive oxygen species in neuronal HT22 cells. *Antioxidants*. **2017**, *6*, https://doi.org/10.3390/antiox6010021
6. Dorszewska, J.; Kowalska, M.; Prendecki, M.; Piekut, T.; Kozłowska, J.; Kozubski, W. Oxidative stress factors in Parkinson's disease. *Neural Regen Res* **2021**, *16*, 1383-1391, https://doi.org/10.4103/1673-5374.300980
7. Shen, Y.; Wu, Q.; Shi, J.; Zhou, S. Regulation of SIRT3 on mitochondrial functions and oxidative stress in Parkinson's disease. *Biomed Pharmacother* **2020**, *132*, 110928,

https://doi.org/10.1016/j.biopha.2020.110928
8. Zang, H.; Yang, W.; Tian, X. Simvastatin in the Treatment of Colorectal Cancer : A Review. Evid Based Complementary Altern Med, **2022**, https://doi.org/10.1155/2022/3827933
9. Jia, CY.; Li, JY.; Hao, GF.; Yang, GF. A drug-likeness toolbox facilitates ADMET study in drug discovery. *Drug Discov Today* **2020**, *25*, 248-258, https://doi.org/10.1016/j.drudis.2019.10.014
10. Shah, FH.; Salman, S.; Idrees, J.; Idrees, F.; Akbar, MY. In silico study of thymohydroquinone interaction with blood-brain barrier disrupting proteins. *Futur Sci OA* **2020**, *6*, https://doi.org/10.2144/fsoa-2020-0115
11. Du, W.; Liang, X.; Wang, S.; Lee, P.; Zhang, Y. The Underlying Mechanism of Paeonia lactiflora Pall. in Parkinson's Disease Based on a Network Pharmacology Approach. *Front Pharmacol* **2020**, *11*. https://doi.org/10.3389/fphar.2020.581984
12. Liu, Y.Y.; Yu, L.H.; Zhang, J.; Xie, D.J.; Zhang, X.X.; Yu, J.M. Network Pharmacology-Based and Molecular Docking-Based Analysis of Suanzaoren Decoction for the Treatment of Parkinson's Disease with Sleep Disorder. *Biomed Res. Int.* **2021**, *2021*, https://doi.org/10.1155/2021/1752570
13. David, TI.; Adelakun, NS.; Omotuyi, OI.; Metibemu, DS.; Ekun, OE.; Eniafe, GO.; et al. Molecular docking analysis of phyto-constituents from Cannabis sativa with pfDHFR. *Bioinformation* **2018**, *14*, 574-579, https://doi.org/10.6026/97320630014574.
14. Gajjar, N.D.; Dhameliya, T.M.; Shah, G.B. In search of RdRp and Mpro inhibitors against SARS CoV-2: Molecular docking, molecular dynamic simulations and ADMET analysis. *J. Mol. Struct.***2021**, *1239*, https://doi.org/10.1016/j.molstruc.2021.130488
15. Qin, H.; Zhang, H.; Zhang, X.; Zhang, S.; Zhu, S.; Wang, H. Resveratrol attenuates radiation enteritis through the SIRT1/FOXO3a and PI3K/AKT signaling pathways. *Biochem. Biophys. Res. Commun*. **2021**, *554*, 199-205, https://doi.org/10.1016/j.bbrc.2021.03.122
16. Bonte, MA.; El Idrissi, F.; Gressier, B.; Devos, D.; Belarbi, K. Protein network exploration prioritizes targets for modulating neuroinflammation in Parkinson's disease. *Int. Immunopharmacol*. **2021**, *95*, 107526. https://doi.org/10.1016/j.intimp.2021.107526
17. Sun, Q.; Kang, RR.; Chen, KG.; Liu, K.; Ma, Z.; Liu, C.; Deng, Y.; Liu, W.; Xu, B. Sirtuin 3 is required for the protective effect of Resveratrol on Manganese-induced disruption of mitochondrial biogenesis in primary cultured neurons. *J. Neurochem*, **2021**, *156*, 121-35, https://doi.org/10.3390/cells7120235
18. Santo, EE.; Paik, J. FOXO in neural cells and diseases of the nervous system. *Curr. Top. Dev. Biol*. **2018**, *127*, 105-18, https://doi.org/10.1016/bs.ctdb.2017.10.002
19. Xiao, B.; Kuruvilla, J.; Tan, EK. Mitophagy and reactive oxygen species interplay in Parkinson's disease. *NPJ Parkinsons Dis*, **2022**, *8*, 1-3, https://doi.org/10.1038/s41531-022-00402-y
20. Du, S.; Zheng, H. Role of FoxO transcription factors in aging and age-related metabolic and neurodegenerative diseases. *Cell Biosci*, **2021**, *11*, 1-7, https://doi.org/10.1186/s13578-021-00700-7
21. Martins, R.; Lithgow, GJ.; Link, W. Long live FOXO: unraveling the role of FOXO proteins in aging and longevity. *Aging cell*, **2016**, *15*, 96-207, https://doi.org/10.1111/acel.12427
22. Kim, TY.; Leem, E.; Lee, JM.; Kim, SR. Control of reactive oxygen species for the prevention of parkinson's disease: The possible application of flavonoids. *Antioxidants*, **2020**, *9*, 583, https://doi.org/10.3390/antiox9070583

Supplementary materials

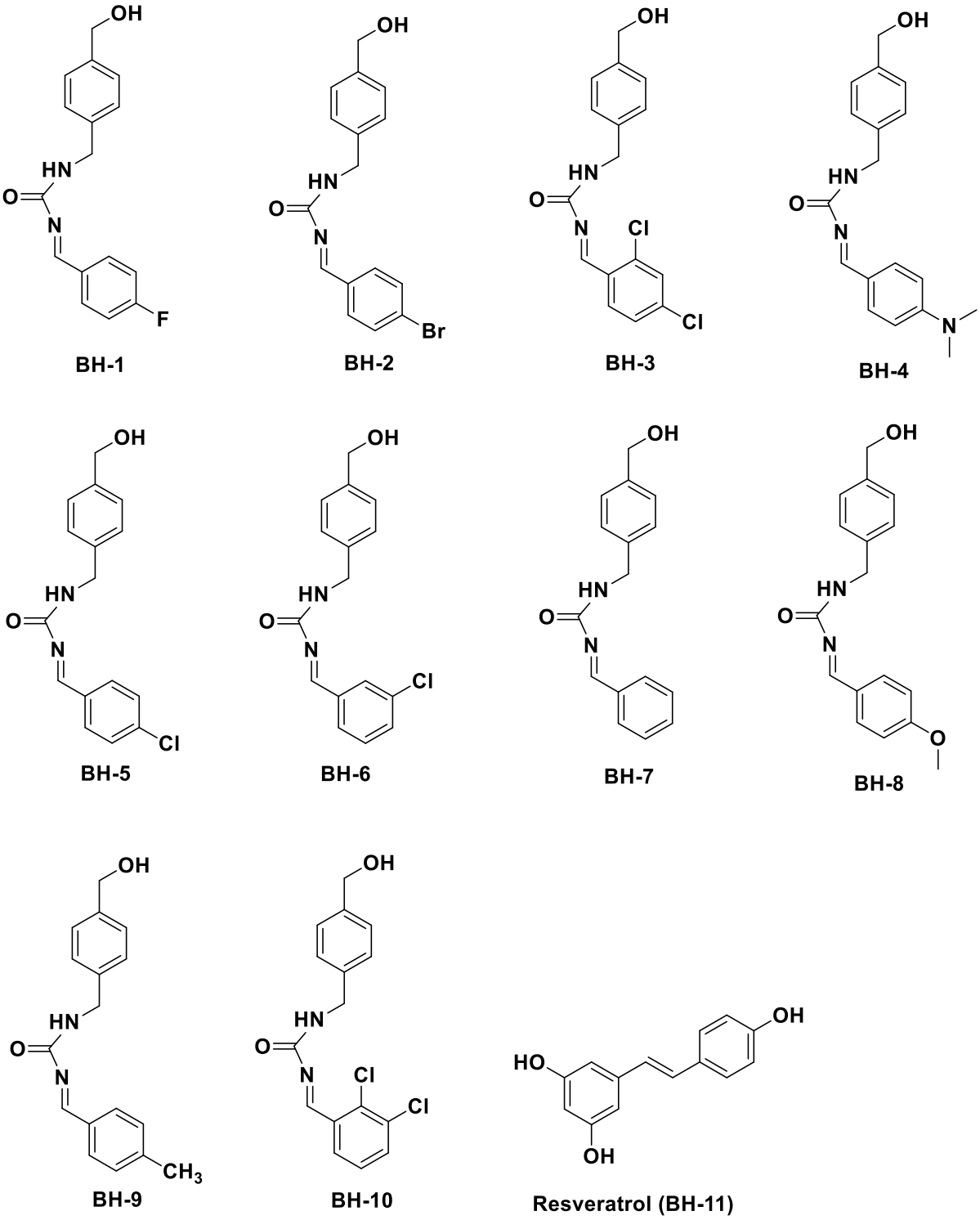

Figure S1. Designed Benzylidene-based hydroxy derivatives BH-1 to BH-11.

Kyoto Encyclopedia of Genes database

For a potential gene enrichment study, the likely genes involved in the progression of Parkinson's disease were searched for in a string database (https://string-db.org/). The KEGG pathways and genes connected to them were examined in the protein interaction network (https://www.genome.jp/kegg/). In Cytoscape 3.7.2, the data were further examined for potential networks between phytoconstituents, genes, and pathways.

Table S1. KEGG pathways and their modulated proteins.

Term ID	Term Description	Observed Gene Count	Background Gene Count	False Discovery Rate	Matching Proteins In Your Network (Labels)SSSSS
hsa04211	Longevity regulating pathway	4	87	1.91	PPARGC1A, FOXO1, FOXO3, SOD2
hsa01200	Carbon metabolism	4	117	1.78	ACSS2, GLUD1, ACSS1, IDH2
hsa01100	Metabolic pathways	6	1447	0.93	FOXO1, SIRT3, IDH2, MAOA, ALOX5, MAOB
hsa04213	Longevity regulating pathway - multiple species	3	61	1.94	FOXO1, FOXO3, SOD2
hsa04068	FoxO signaling pathway	9	127	1.16	SIRT3, PRKAB1, CREBBP, PRKAA2, FOXO1, SOD2, PPARGC1A, SOD1, CREB1
hsa04152	AMPK signaling pathway	3	120	1.65	PPARGC1A, FOXO1, FOXO3
hsa00630	Glyoxylate and dicarboxylate metabolism	2	30	2.07	ACSS2, ACSS1
hsa00620	Pyruvate metabolism	2	38	1.97	ACSS2, ACSS1
hsa00640	Propanoate metabolism	2	34	2.02	ACSS2, ACSS1
hsa04728	Dopaminergic synapse	4	112	0.0029	DRD4, MAOA, FOXO1, MAOB
hsa05016	Huntington disease	3	298	1.25	PPARGC1A, NDUFA9, SOD2
hsa00010	Glycolysis / Gluconeogenesis	2	65	1.74	ACSS2, ACSS1
hsa05230	Central carbon metabolism in cancer	2	69	1.71	IDH2, SIRT3
hsa04146	Peroxisome	5	79	1.65	SOD1, IDH2, FOXO1, SIRT3, SOD2
hsa04922	Glucagon signaling pathway	2	101	1.55	PPARGC1A, FOXO1
hsa04931	Insulin resistance	2	133	1.43	PPARGC1A, FOXO1
hsa04910	Insulin signaling pathway	6	107	1.52	PPARGC1A, MTOR, PRKAA2, FOXO1, PPARA, CREB1S

Table S2. Designed Benzylidene-based hydroxy derivatives BH-1 to BH-10 with their their SMILES.

Compounds code	Substituted (R)-Aldehydes	SMILES
BH-1	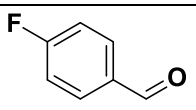	O=C(N=Cc1ccc(F)cc1)NCc2ccc(CO)cc2

Compounds code	Substituted (R)-Aldehydes	SMILES
BH-2	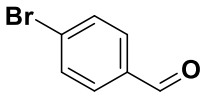	O=C(N=Cc1ccc(Br)cc1)NCc2ccc(CO)cc2
BH-3	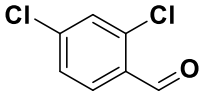	O=C(N=Cc1ccc(Cl)cc1Cl)NCc2ccc(CO)cc2
BH-4	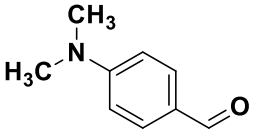	CN(C)c2ccc(C=NC(=O)NCc1ccc(CO)cc1)cc2
BH-5	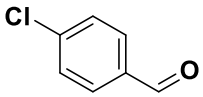	O=C(N=Cc1ccc(Cl)cc1)NCc2ccc(CO)cc2
BH-6	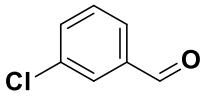	O=C(N=Cc1cccc(Cl)c1)NCc2ccc(CO)cc2
BH-7	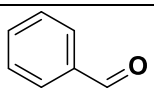	O=C(N=Cc1ccccc1)NCc2ccc(CO)cc2
BH-8	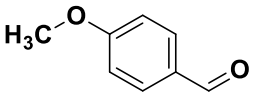	COc2ccc(C=NC(=O)NCc1ccc(CO)cc1)cc2
BH-9	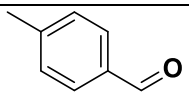	Cc2ccc(C=NC(=O)NCc1ccc(CO)cc1)cc2
BH-10	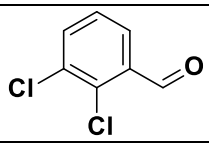	O=C(N=Cc1cccc(Cl)c1Cl)NCc2ccc(CO)cc2
BH-11	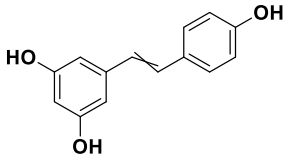	C1=CC(=CC=C1C=CC2=CC(=CC(=C2)O)O)O

Molecular docking

The research was conducted out in Schrödinger suite 2022, which consists of many modules. The ligands were created using the LigPrep module, and the energy of the ligands was minimized using the Epik module and the OPLS3 force field. The ZINC database (https://zinc.docking.org/) was used in the construction of the ligands. The protein, which is a human sirtuin 3 coupled to the Ac-ACS peptide and Carba-NAD, was retrieved from the Protein Data Bank at (https://www.rcsb.org/), using the PDB ID: 4FVT. The process of preparing protein involved a protein preparation module, which cleared unwanted residual heteroatoms and water molecules before adding the missing amino acid residues and adding partial charges to each atom using the OPLS3 force field. The receptor grid generation option was utilized to prepare the gliding module using a grid box, and a grid box was formed for the docking. For the docking between proteins and energy-minimized ligands in the mol format the extra precision (XP) approach was used, and a further Ligand Docking module was established to obtain the best binding interaction. The glide XP visualizer was used to assess the docking findings. Amino acid residues and the highest docking, glide, and MMGBSA values were examined.

Table S3. Molecular docking results of BH-1 to BH-11 with the PDB ID: 4FVT.

Sr. No.	Compound Name	Docking score (kcal/mol)	H-bond interactions	Hydrophobic interactions	Halogen Interactions	MMGBSA (kcal/mol)A
1	BH-1	-7.463	ILE 230 ILE 154	PHE 294	-	-59.55
2	BH-2	-6.909	ILE 230 ILE 154	PHE 294	-	-32.48
3	BH-3	-6.584	THR320 SER321	HIS 248 PHE 294	-	-51.58
4	BH-4	-6.327	HIS 248 PHE 294	PHE 294	-	-27.62
5	BH-5	-5.769	THR 320 SER 321 ASN 341	HIS 248	-	-50.24
6	BH-6	-5.753	THR 320 SER 321 ASN 344	HIS 248 ALA 146	-	-51.49
7	BH-7	-5.632	THR 320 SER 321 GLN 228	PHE 180	-	-35.54
8	BH-8	-5.503	THR 320 SER 321 ASN344 HIS 248	-	-	-48.57
9	BH-9	-5.284	ARG 158 ASP 156	-	-	-52.41
10	BH-10	-5.021	THR 320 SER 321	HIS 248	ASN 229	-51.44
11	BH-11	-4.037	VAL 292 PRO 1555	PHE 294 PHE 180 HIS248	-	-15.61

H-bond interaction Hydrogen bond interactions, MMGBSA molecular mechanics generalized born surface area

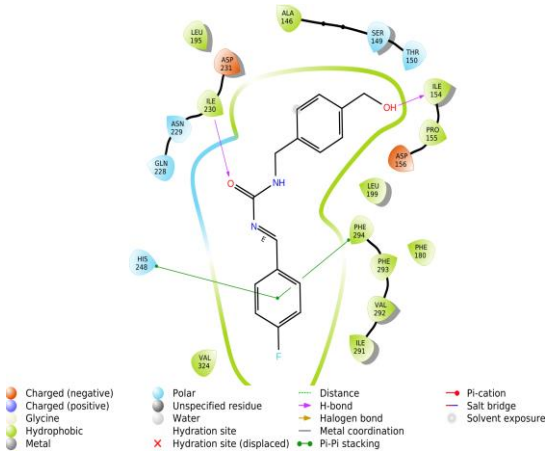

BH-1

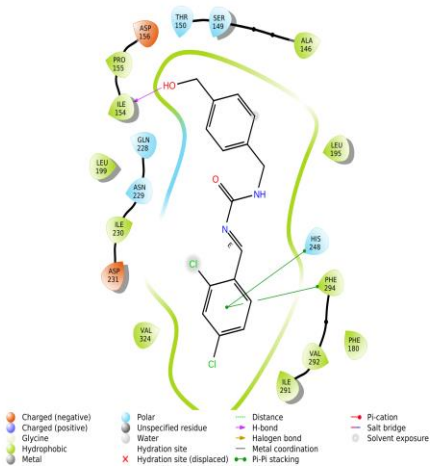

BH-3

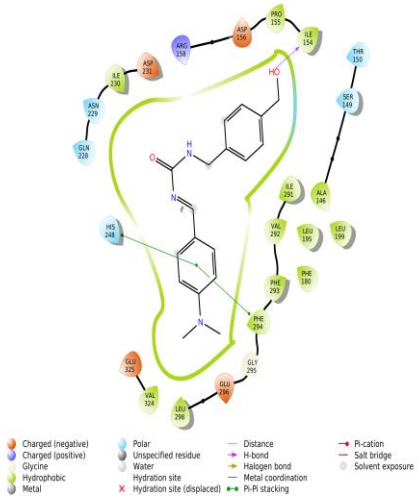

BH-4

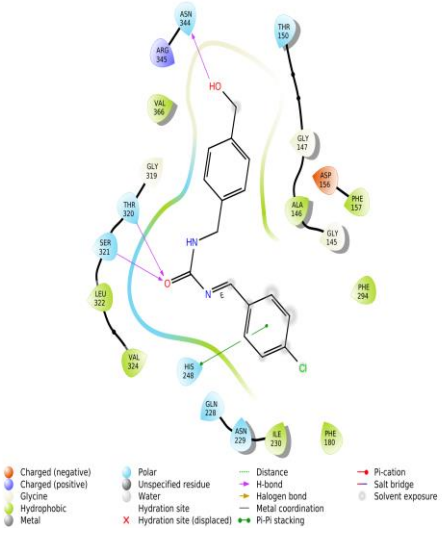

BH-5

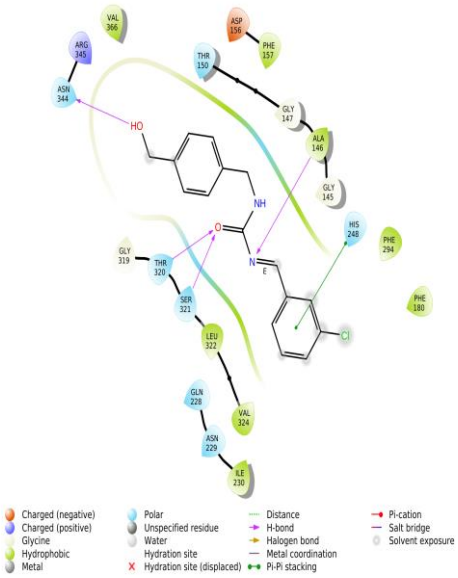

BH-6

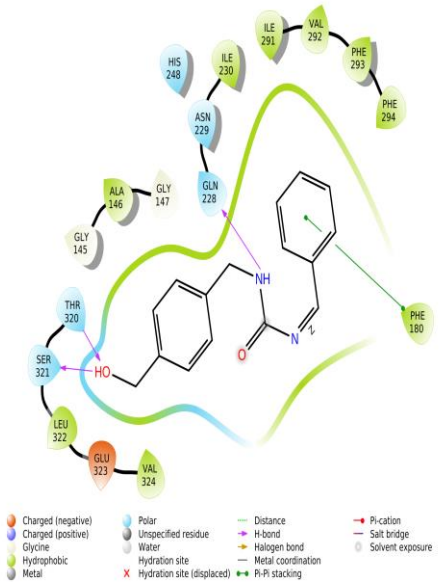

BH-7

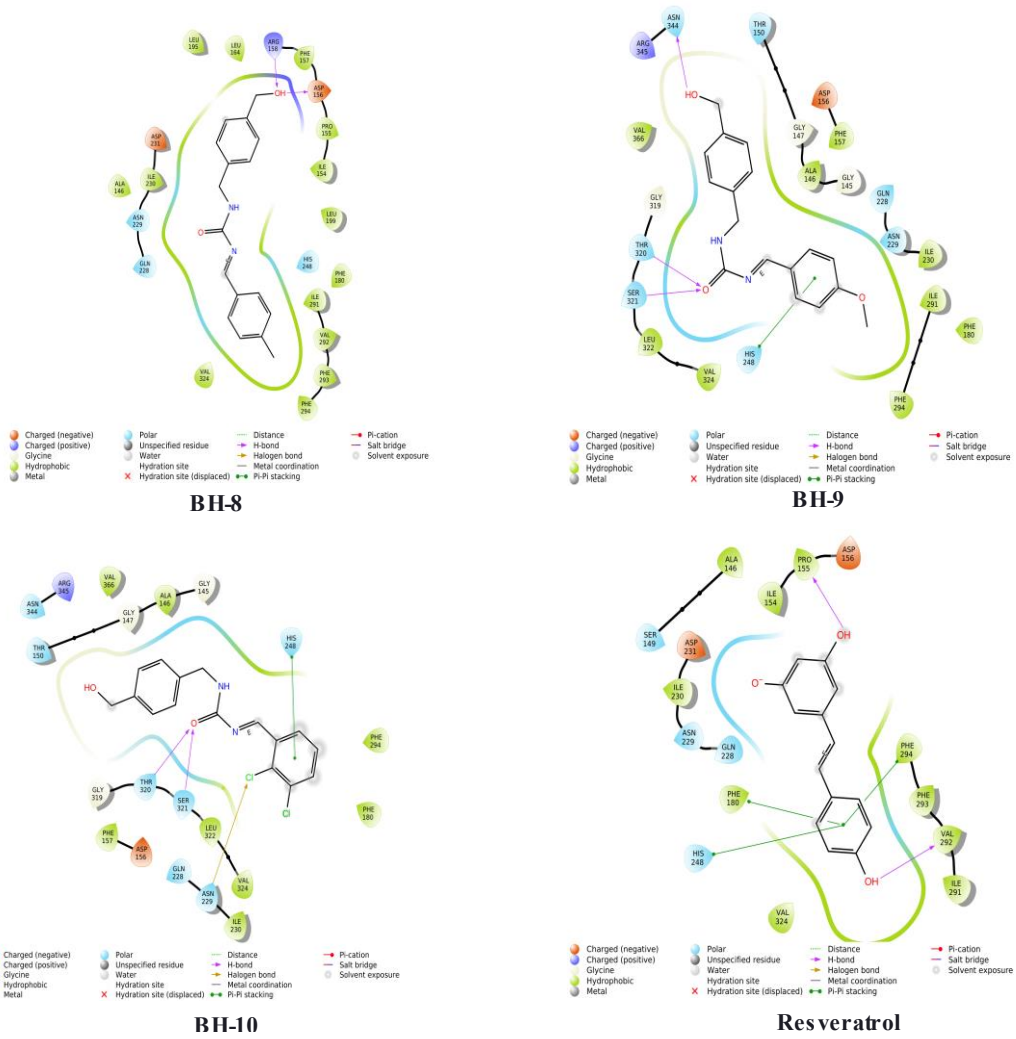

Figure S2. Two-dimensional interactions between BH-1 to BH-10 and resveratrol with sirtuin 3 (PDB ID: 4FVT).

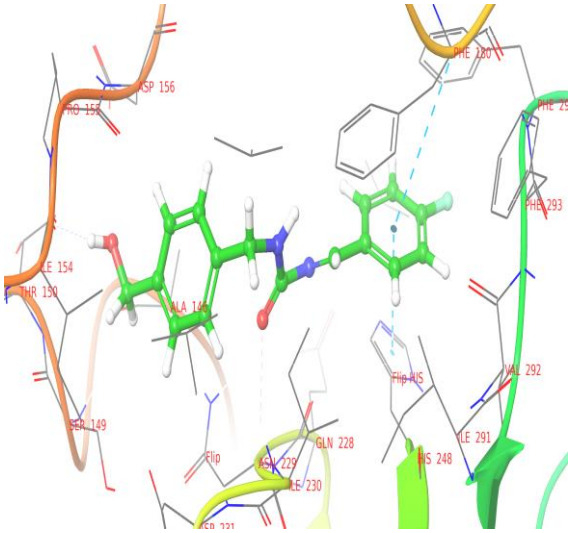

BH-1

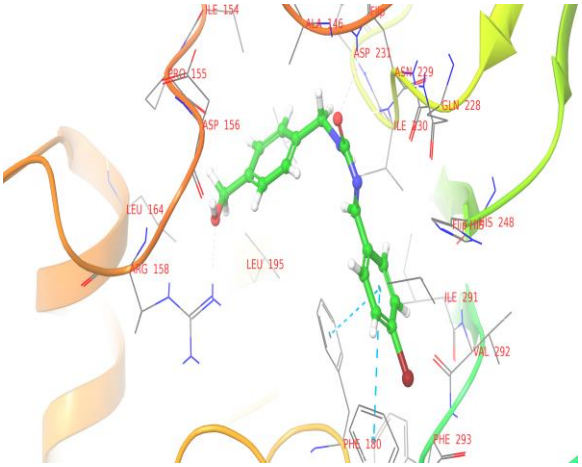

BH-2

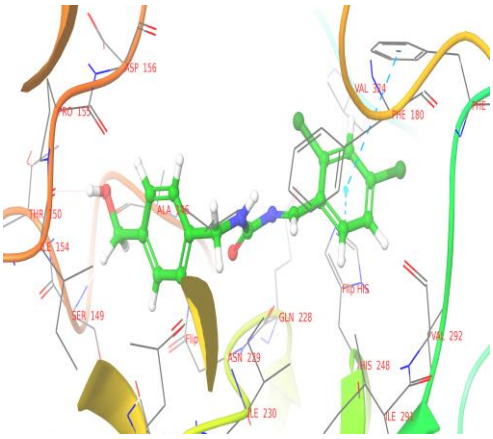

BH-3

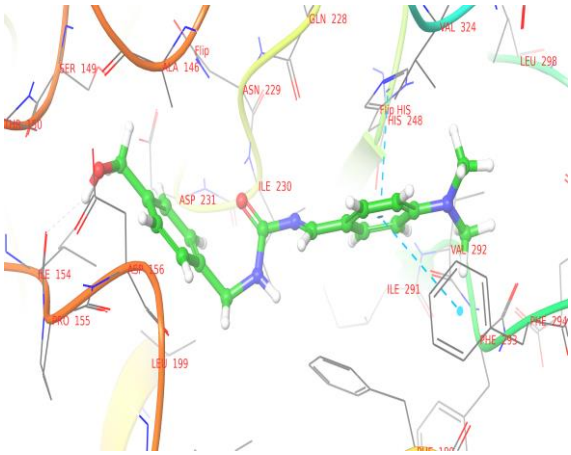

BH-4

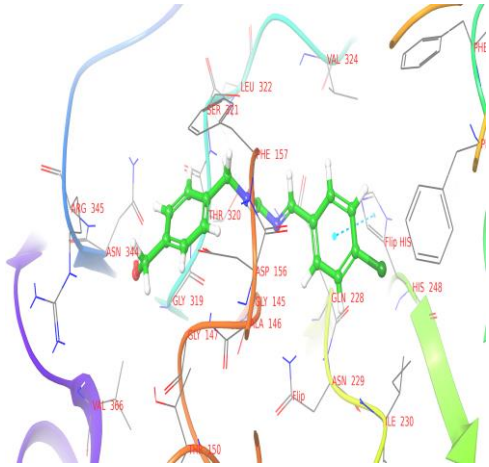

BH-5

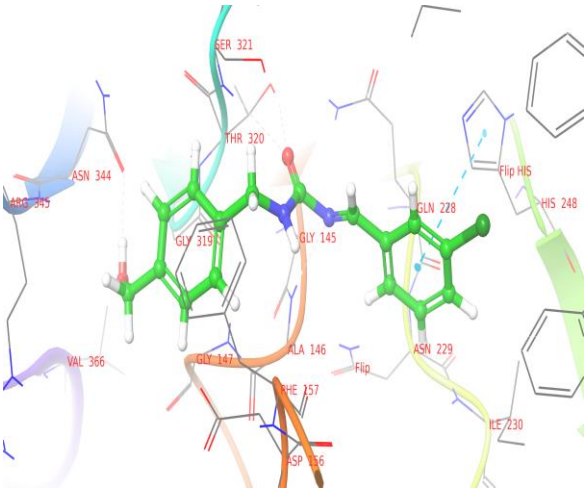

BH-6

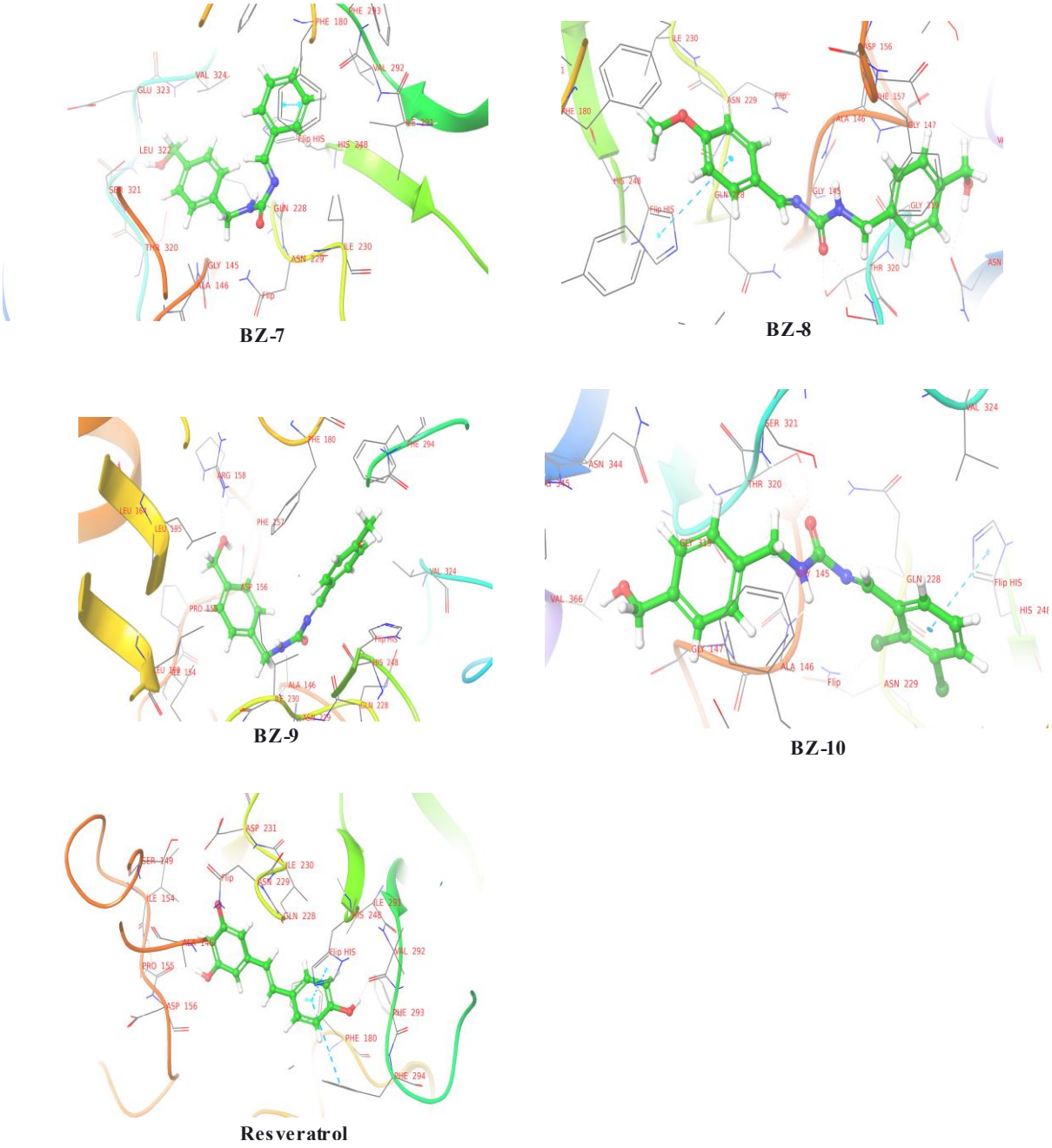

Figure S3. Three-dimensional interactions between BZ-1 to BZ-14 and resveratrol with sirtuin 3 (PDB ID: 4FVT).